Naveed, Nida and Anwar, Muhammad Naveed (2024) Optimising 3D Printing Parameters through Experimental Techniques and ANOVA-Based Statistical Analysis. SPE Polymers. ISSN 2690-3857

Downloaded from: http://sure.sunderland.ac.uk/id/eprint/17306/

Usage guidelines

Please refer to the usage guidelines at http://sure.sunderland.ac.uk/policies.html or alternatively contact sure@sunderland.ac.uk.

Optimising 3D Printing Parameters through Experimental Techniques and ANOVA-Based Statistical Analysis

[1]Nida Naveed, [2]Muhammad Naveed Anwar

[1]Faculty of Technology, University of Sunderland UK

[2]Faculty of Engineering and Environment, Northumbria University, UK

ABSTRACT

Additive Manufacturing (AM) has revolutionised the manufacturing industry by enabling the fabrication of complex geometries and designs with ease. 3D printing - Fused Deposition Modelling (FDM) has emerged as a prevalent technique, owing to its versatility and cost-effectiveness. However, the FDM process is complex and depends on multiple parameters, which makes it challenging to obtain high-quality and consistent 3D printed components. The purpose of this study is to simplify the printing process for users and potentially improve the overall quality and consistency of printed objects. This research delved into optimising 3D printing parameters, specifically raster orientation and in-fill speed, for PLA material through three experimental studies. The mean effect of these parameters and the effects of their interaction through analysis of variance (ANOVA) on tensile properties were also discussed. Initial experiments identified the most suitable parameters and its optimal values for PLA, which were then applied to five different materials: PETG, PLA tough, Recycle PLA, Plain PLA, and ABS. Tensile tests assessed the printed parts, and Scanning Electron Microscopy (SEM) was employed to analyse fracture interfaces and material failure causes. This study identified a raster of 45°/ -45° and 30 mm/sec infill speed as optimal for diverse 3D printing materials. Notably, ABS, PETG, and tough PLA exhibited better tensile strengths, surpassing manufacturer benchmarks. However, Plain PLA and Recycled PLA, despite lower tensile strengths, proved valuable for specific applications. Interestingly, all tested materials showed greater flexibility than manufacturer recommendations, suggesting their suitability in scenarios needing both strength and flexibility. This study's results offer promising avenues for refining 3D printing practices, to the advantage of all users. The findings from this study offer significant insights for future research to investigate the effect of other process parameters on the quality of 3D printed parts, leading to further advancements of AM.

Highlights

- Optimised 3D printing parameters.
- Applicability of optimised settings extended across various materials.
- ABS, PETG, and tough PLA exceeded manufacturer benchmarks in tensile strength.
- Experimental and ANOVA findings are in good agreement, revealing significant process parameters.

Keywords: Fused deposition modelling (FDM), raster orientation, infill speed, 3D printer.

Introduction

3D printing with Fused Deposition Modelling (FDM) is one of the popular techniques in advanced additive manufacturing (AM). It constructs objects by layering and depositing multiple thin layers. By using these techniques objects can produce with a good range of materials such as polymers, composites and metals. First, the design can be generated digitally with CAD software and then transferred to the 3D printer for a physical creation [1–3]. 3D printing offers the unique ability to produce intricate designs with detailed internal characteristics, which are challenging to achieve with traditional manufacturing methods [4]. Using a 3D printer, parts can be printed using multiple materials in a single process, offering distinct material characteristics tailored for specific applications [5, 6]. Materials utilised in additive manufacturing can be recycled and repurposed for various applications, aiding in the reduction of environmental harm and resource consumption [7–9]. Nevertheless, several hurdles hinder the widespread adoption of this method, including high equipment costs, limited knowledge of the AM process, restricted material availability, production costs, and a scarcity of in-house AM resources [10, 11]. Addressing these challenges necessitates a comprehensive examination of the AM process and its manufacturing approach to discern potential innovations. Consequently, significant research is essential to enhance the performance of products derived from this method and expand its applications.

There are a range of polymers that can be used with FDM 3D printers [12, 13]. Polylactide (PLA) is a bioactive, biodegradable material made up with renewable resources such as maize starch, tapioca roots, and sugarcane. Common in 3D printing, it's chosen for its low melting point and user-friendliness, serving as a primary material for prototypes, models, and complex parts. Its biocompatibility makes it suitable for food packaging, medical implants, and other biomedical uses [14]. While eco-friendly when discarded correctly, PLA's unsuitability for high-temperature settings and potential durability concerns in certain uses limit its applicability. ABS, or Acrylonitrile Butadiene Styrene, is a robust thermoplastic formed with acrylonitrile, butadiene, and styrene. It is widely used in 3D printing, electronics, toys, appliances, and cars, ABS is favoured for its strength, heat and chemical resistance, and ease of fabrication [15]. PETG (Polyethylene Terephthalate Glycol) is a versatile thermoplastic polyester favoured in 3D printing for its usability. It's transparent, durable, and lightweight with notable impact and chemical resistance. Withstanding UV light and moisture, it's optimal for outdoor use and humid areas. Often chosen for food containers, water bottles, and medical equipment due to its safety and biocompatibility, PETG in 3D printing ensures accurate and smooth parts. Its low melting point makes it suitable for most FDM 3D printers [15]. Tough PLA is similar to PLA but boasts ABS-like toughness and superior impact resistance. It flexes before breaking, making it ideal for engineering tasks demanding high-wear and impact resistance. Similar to regular PLA, it should not face temperatures over 60°C due to its low thermal expansion coefficient. Its enhanced impact resistance and improved toughness are vital for expanding its applications in engineering [16, 17].

FDM is a notable AM technique in 3D printing, it allows for the creation of complex geometries that may be challenging or costly to produce with other conventional methods. The additive nature of 3D printing also contributes to reduced material waste, as it only deposits material where needed, minimising excess and optimising material usage [5, 18]. Contrastingly, FDM exhibits certain drawbacks, including lower accuracy when compared to alternative 3D printing technologies [19]. This decreased precision is constrained by factors such as the nozzle size and the specific filament in use. The layered approach of FDM contributes to a noticeable layering effect on the final products, impacting the smoothness of their surfaces. Weakness in part bonding can further result in diminished strength [20, 21]. Moreover, FDM faces challenges in achieving precision, especially with smaller and intricate components, impacting the overall quality of the printed object. Strengthening FDM parts involves adjusting infill patterns and density for an improved internal structure [22]. Optimising process parameters is key to enhancing layer adhesion and overall strength in 3D printed parts [23]. FDM's complexity arises from multiple influencing parameters [24, 25]. These can be grouped into four: part deposition parameters (including infill pattern, speed, layer width, thickness, and raster details), machine settings (such as nozzle temperature and print bed temperature), filament characteristics (including density and colour), and environmental aspects such as temperature and humidity [26]. Another study investigated the impact of bed temperature, primary layer thickness, and infill patterns on 3D printed part mechanical properties. Employing Fused Deposition Modelling, the study uncovers that bed temperature influences strength, increasing and then decreasing. Primary layer thickness correlates positively with strength, and triangular/honeycomb infill patterns outperform. The findings provide crucial insights for optimising 3D printing processes and enhancing mechanical properties [27]. Literature reviews highlight that minor shifts in these parameters can greatly impact part quality.

To ensure the printed part's optimal properties, it is important to study the effects of these process parameters on the part's material properties, aiming for improving quality through most suitable settings.

There are some studies performed to identify the suitable process parameters for the 3D printing parts. It has been explored that the mechanical properties of any material and its porosity can be significantly affected by air gap and raster width [28]. Other authors highlighted that there are five parameters that have a greater effect on the quality of 3D printed parts: raster angle and its width, layer width and its orientation, and air gap. Raster angle is the direction of the raster relative to the x-axis of the build table [29]. Raster width is the width of the raster pattern used to fill interior regions of a part. Layer width is the thickness of each layer of material deposited by the 3D printer. The layer orientation indicates the alignment of these layers along specific axes, affecting the anisotropic properties of the printed material [30]. Air gap is the gap between two adjacent rasters on the same layer. Infill speed refers to the speed at which the 3D printer deposits material to fill the interior structure of a printed object [29]. In some studies, the different raster angles were investigated and found that the 45°/-45° filament placement provided some good results [31]. Similarly, in one another study, author [32] investigated the different placement filament raster angles provided a better strength. In another study, it has been identified that the raster angles 45° and 90° give the strongest parts. However, it also identified imperfections in 3D printed samples [33]. In another study, the author explored other FDM parameters for PEEK and found that nozzle temperature has significant effects on roughness and elastic modulus as well as layer height [34].

Existing research provides valuable insights into 3D printing settings, yet a critical gap persists. The need for systematic exploration arises to ascertain the universal efficacy of identified parameters across a diverse array of 3D printing materials. Existing studies predominantly focus on specific materials, limiting generalisability. A standardised framework for evaluating settings across materials is absent, hindering the synthesis of collective knowledge and best practices. To address this, a comprehensive research initiative is essential, aiming to determine optimal 3D printing settings applicable universally.

In the current study the effort has been made to perform a systematic study to optimise the 3D printing process parameters. This paper discussed the results of number of experimental studies that used to optimise 3D printing parameters, specifically raster orientation and in-fill speed and simplify the printing process for users and potentially improve the overall quality and consistency of printed objects. Initial experiments identified the ideal parameters for PLA, which were then applied to five different materials: PETG, PLA tough, Recycle PLA, Plain PLA, and ABS. Tensile tests assessed the printed parts, and SEM was employed for detailed micrography to analyse fracture interfaces and material failure causes.

Experimental procedures

First, the standardised tensile test samples were prepared using a 3D printer and then, tensile testing of 3D printed samples were performed. After testing, the detailed microstructural analysis was performed to examine the outer and inner surfaces of 3D printed samples. These steps are discussed below in detail.

Fabrication of 3D printed samples:

This study utilised the Ultimaker-2 3D printer, employing the Fused Deposition Modelling (FDM) technique. In FDM printing, a thermoplastic material undergoes melting and extrusion through a nozzle, subsequently being deposited layer by layer to form a three-dimensional object.to fabricate the 3D printed samples. To fabricate these samples, firstly, the digital model of the sample was created using CAD SolidWorks 2018 software according to the ASTM D638 standard [35]. Then, this virtual sample geometry was transferred to Cura4.3.0 – 3D printing software in STL format to prepare the design. To facilitate the printing process, personalised printing configurations were employed through this software that allows precise adjustment of printing parameters on the printer. In this study three sets of experiments are performed, and their results are discussed in detail.

Results and Discussions

First experiment

For the first experiment, the PLA 3D printing material was used to print the samples. These samples were extruded at speed of 65 to 70mm/s at 200 °C. The bed surface temperature 60 °C was used for these prints. The samples were fabricated with seven different settings of raster angles (part build orientation) *[36]* including 0°, 30°, 45°, 60°, 90°, 45°/-45° and 0/90° one after the other. For these sample printing, the solid fill (100% infill density) was used for each raster setting. Examining a 3D-printed material with 100% infill offers valuable insights into its ultimate strength and durability. To assess the integrity of a part, it is beneficial to investigate the impact of 100% infill on the stiffness, stability, and overall performance of 3D-printed objects [37]. The printing of the first set of samples was performed

at a high speed of 70 mm/s to initiate the study. The process parameters details are shown in Table 1. Each configuration produced three identical tensile samples, resulting in a total of 21 PLA printed samples [28]. The mechanical tests were performed at a speed of 5 mm/min for all these samples.

Table 1: shows the details of 3D printing process parameters used for the first experiment.

3D printing process parameters	
Raster orientation angles	0°, 30°, 45°, 60°, 90°, 45°/-45° and 0/90°
Infill speeds	70 mm/s
Infill density	100%
Infill layer thickness	0.1 mm
Bed temperature	60 °C
Extruded temperature	200 °C

The stress-strain plots for all the samples printed with all seven different raster angles were presented in Figure 1 a. These plots show different material behaviour for each parameter setting which includes strongest, toughest and brittle behaviour. The stress value at the point of fracture was compared among all samples to identify the strongest sample and its corresponding process parameters. Notably, the 45°/-45° orientation exhibited the highest strength, reaching 59 MPa, while the 0° orientation resulted in the weakest sample with a stress value of 14.03 MPa. Samples printed with orientations of 30° and 0° broke without significant plastic deformation when subjected to stress and exhibited brittle material behaviours. Additionally, the graph indicates that the 45°/-45° orientation yielded a sample with high toughness, whereas the toughness values decreased sequentially from 45° to 0/90°, 90°, 30°, 60°, and 0° orientations. Toughness is an indicator of a material's capacity to absorb energy prior to fracturing, and it is measured by assessing the area beneath the stress-strain curve. Figure 1 also illustrates the influence of the raster settings on PLA material mechanical properties, encompassing tensile strength, modulus of elasticity, and elongation at break. The 45°/-45° raster angle yielded the most robust sample, averaging 59 MPa in tensile strength and exhibiting the highest elongation at 6.5%. Raster angle of 45° and 0/90° produced samples with average tensile strengths of 56 MPa and 41 MPa, respectively, representing the second and third highest strengths (8% and 30% lower than the 45°/-45°, respectively) among all printed samples. In contrast, the 0°, 30°, and 60° orientations resulted in weaker samples, displaying average ultimate strengths of 14.04 MPa, 17.11 MPa, and 15.27 MPa, respectively. These findings highlight the significance of raster position as a critical parameter in 3D printing, playing a vital role in determining specimen strength. Similar trends were found for the material properties of elongation at break and the samples printed with 45°/-45° raster orientation performed best. A 45°/-45° raster angle in 3D printing enhances strength through optimal interlayer bonding, reducing anisotropy, resisting delamination, facilitating effective load distribution, and ensuring balanced material usage. This diagonal orientation fosters robust layer adhesion, minimising preferential axes for strength. It mitigates delamination risks, promoting cohesive structures and uniform load transfer during stress. The balance between X and Y axes minimises anisotropic effects, enhancing overall structural integrity. Additionally, the pattern allows for more efficient material usage, contributing to better tensile strength and mechanical performance in printed objects.

In addition to this, Modulus of Elasticity for these samples, the 90° raster orientation yielded a value of 1.7 GPa, while the 45° orientation resulted in 1.5 GPa. On the other hand, the 0/90° and 45°/-45° orientations registered values of 1.2 GPa and 1.1 GPa respectively. Therefore, the samples produced with 90° and 45° raster orientations demonstrated greater stiffness compared to the other orientations. Therefore, for applications requiring high tensile strength, the 0/90° and 45°/-45° raster orientations are the more suitable choices. However, its influence on strength requires further investigation, especially when considering raster orientation in combination with other printing parameters such as infill speed.

The material strength is closely tied to its internal composition at micron level. Therefore, examining the changes in internal composition of the fracture surfaces is crucial for understanding the causes of the failure and its mechanisms of the material. The fracture interfaces of the tensile test samples were investigated in this study. Additionally, the external surfaces of these samples were studied to detect any flaws that might have occurred during the 3D printing process. A Hitachi S-3000N SEM, operating at an acceleration of 5 KV in a high-vacuum mode, was employed for microstructure analysis. To ready the surfaces for SEM scrutiny, they were fragmented into smaller pieces along their broken surfaces. To mitigate the surface's charging effects, these fragments were then coated with a fine layer of a gold-palladium. This is crucial because it ensures a consistent surface suitable for detailed examination and

capturing good images [38]. The surface made up with the raster angles of 45° and 45°/-45° display outer surfaces without any defect. However, when examining the fractured surfaces across all raster angles, various imperfections such as empty spaces, cracks and openings are evident, as illustrated in Figure 2. Figure 3 shows the SEM imaging reveals defects documented on both the fractured and outer surfaces of the 3D-printed samples, ranging from 39 microns to 1.34 mm. By addressing and preventing these printing imperfections, the quality, strength and precision of 3D parts can be enhanced.

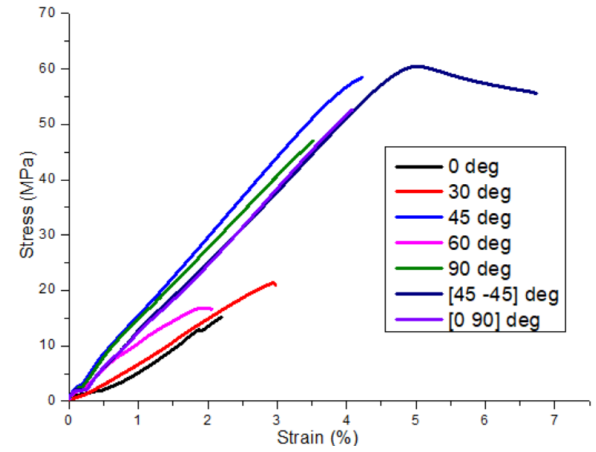

(a) Stress-strain curves

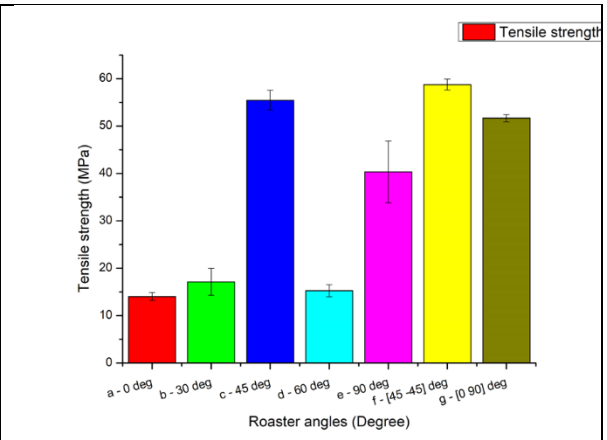

(b) Tensile strength.

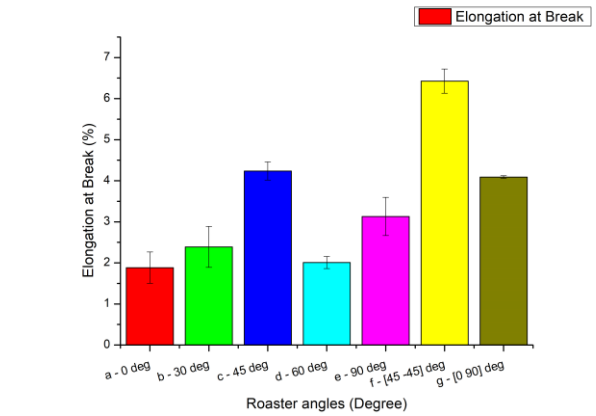

(c) Elongation at break.

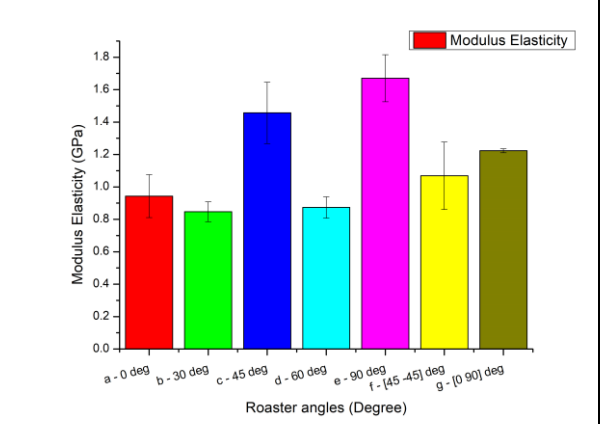

(d) Modulus of elasticity.

Figure 1 shows material properties of 3D printed samples with seven different raster orientations in the experiment 1

a	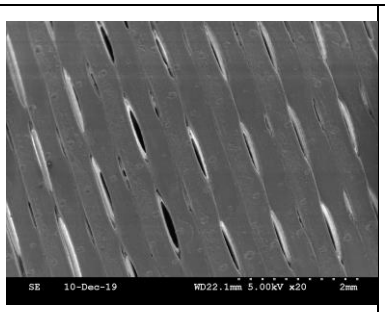	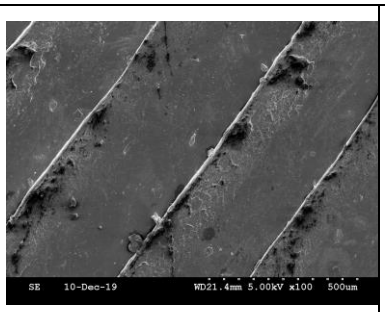	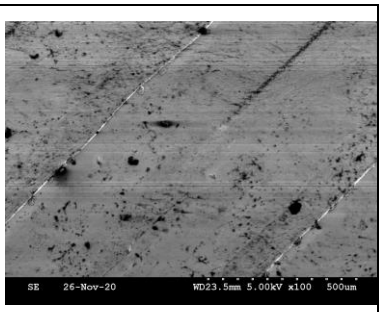
	Raster angle 60°	Raster angle 45°	Raster angle 45°/-45°
b	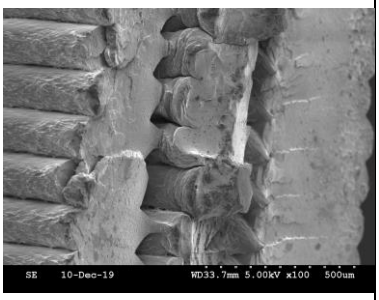	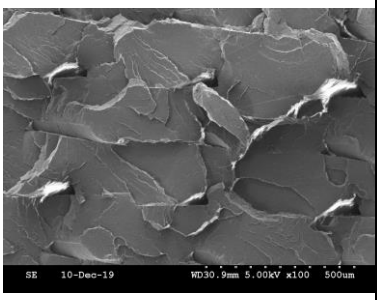	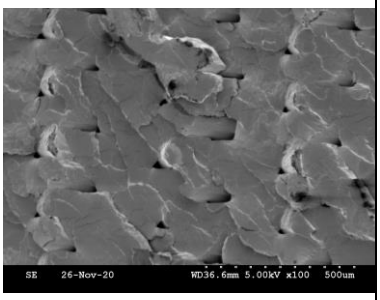
	Raster angle 60°	Raster angle 45°	Raster angle 45°/-45°

Figure 2: SEM images (a) outer surfaces and (b) fractured surfaces.

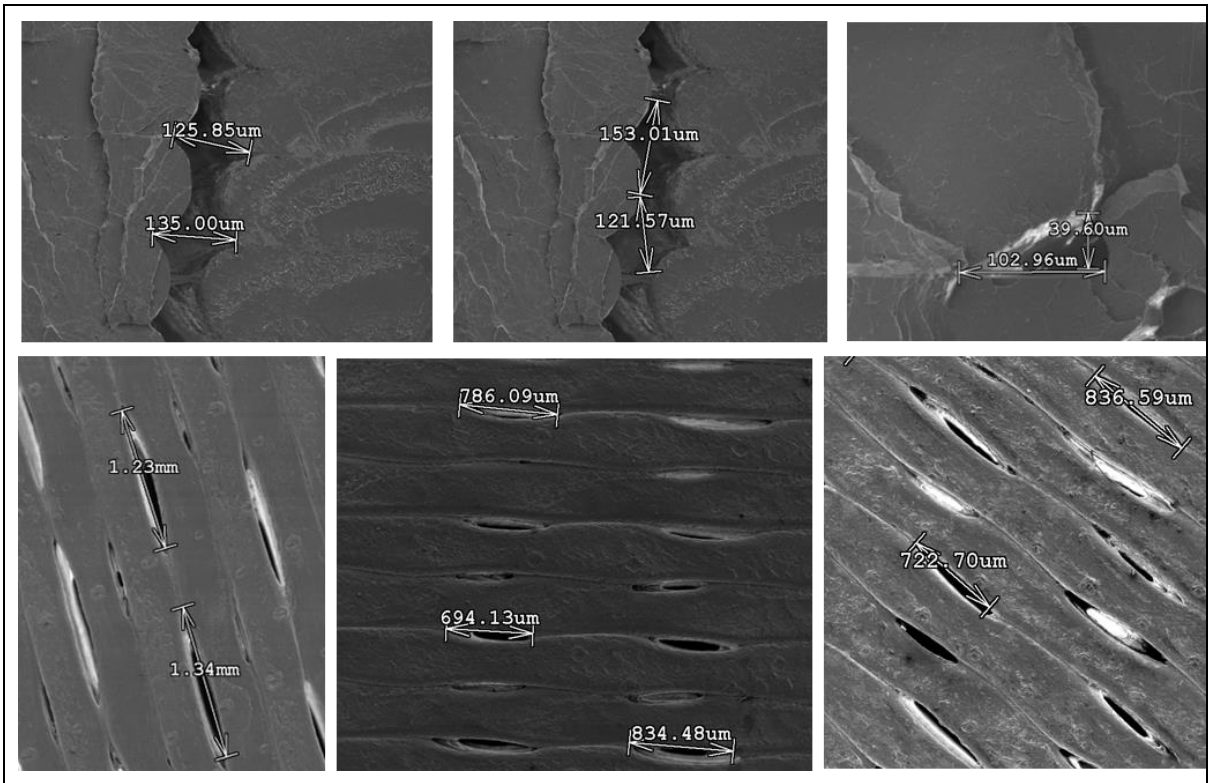

Figure 3: The defects observed during SEM imaging were documented on both the fractured and outer surfaces of the 3D-printed samples.

Second Experiment

Based on the result of the first experiment, the second experiment was designed to print the samples with two raster orientation angles 45°/- 45° and 0°/90° using 35, 50 and 65 mm/s infill speeds of one after the other. The infill speed stands out as a crucial factor in the FDM 3D printing process. It denotes the rate at which the nozzle moves in relation to the print bed, determining both the extruded filament's volume and the cross-sectional geometry of the printed object. All other printing parameters are the same as the first experiment. The PLA was extruded at 200 °C on this 3D printer, with the heated bed set at 60 °C. A 100% infill density and 0.1 mm infill layer thickness were applied for each raster orientation. A total of 18 samples were printed, with three identical tensile samples produced for each combination of the specified parameters (as shown in Table 2). All samples were constructed using 750g spools of PLA material. Subsequently, following sample preparation, the 3D printed samples underwent testing in accordance with the ASTM D638 standard, using a Universal tensile testing machine, following the same procedure as the initial experiment.

Table 2: shows the details of 3D printing process parameters used for second experiment.

3D printing process parameters	
raster orientation angles	45°/- 45° and 0°/90°
infill speeds	35, 50 and 65 mm/s
infill density	100%
infill layer thickness	0.1 mm
Bed temperature	60 °C
Extruded temperature	200 °C

Figure 4 shows the stress-strain curves for these samples. Notably, the PLA material exhibited a substantial stress peak in samples printed with a 45°/- 45° raster angles and an infill speed of 30 mm/s, resulting in robust specimens. As the raster orientation transitions from 45°/- 45° to 0°/ 90° and the infill speed escalates from 35 mm/s to 65 mm/s, these stress peaks diminish. Additionally, there is observable evidence indicating a decrease in sample toughness with the increase in infill speed.

Figure 5 to Figure 7 illustrate the results of the tensile tests, showcasing the impact of raster orientations and infill speeds on various tensile properties of PLA, including tensile strength, modulus of elasticity, and elongation at break. Specifically, the 45°/ - 45° raster orientation at an infill speed of 35 mm/s yielded robust samples with an average tensile strength of 65 MPa and an elongation of 6.8%. In contrast, the 0°/90° raster orientations at the same 35 mm/s infill speed resulted in samples with an average tensile strength of 60 MPa (8% lower than the strength of 45°/- 45° samples at the same speed) and an elongation of 5.9%. Notably, it is observed that the infill speed of 35 mm/s produced the strongest samples with low stiffness, and the tensile strength value decreases as the infill speed increases. One plausible explanation is that lower infill speeds lead to extended deposition times. This prolonged duration facilitates stronger bonding between adjacent layers, resulting in improved tensile properties. These findings demonstrate a 14% enhancement in tensile strength and a notable 36% improvement in elongation when utilising the 45°/- 45° raster orientation and a 35 mm/s infill speed, as compared to the initial experiment. It can be concluded that, in this study, the combination of a 45°/- 45° raster orientation and an infill speed of 35 mm/s represents the most optimal configuration for achieving high tensile strength. These conclusions align well with the previously presented results [30]. On the other hand, it can also be observed that the 45°/- 45° raster angle produced the strongest samples of all three infill speeds and there is very little difference in strengths with other infill speeds. It can also be concluded that the raster angle has much more effects on strength compared to the infill speed. Further investigation can be conducted through examinations of the fractured interfaces in these samples using SEM, and also through analysis of variance (ANOVA) on tensile properties.

The SEM images reveal that samples created with raster angles of 45°/- 45° and 0/90° have compact outer surfaces, and no defects are visible on these surfaces, as seen in Figure 8. This observation aligns with previous findings for other raster angles [16]. Consequently, these two raster angles yield a better surface finish. Nonetheless, some internal defects are apparent on the fractured interfaces of these samples. These defects are evident in the form of apparent imperfections, notably empty spaces and openings. The sizes of these openings range from 65 microns to 19 microns, showcasing improvement compared to the results of the first experiment. Nevertheless, their presence persists. Understanding and addressing these internal flaws are crucial for further optimising the printing process and ensuring the production of high-quality components with enhanced mechanical properties.

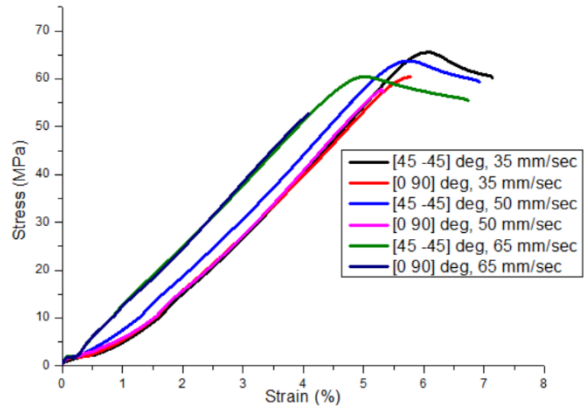

Figure 4: Stress-strain curves for all the samples

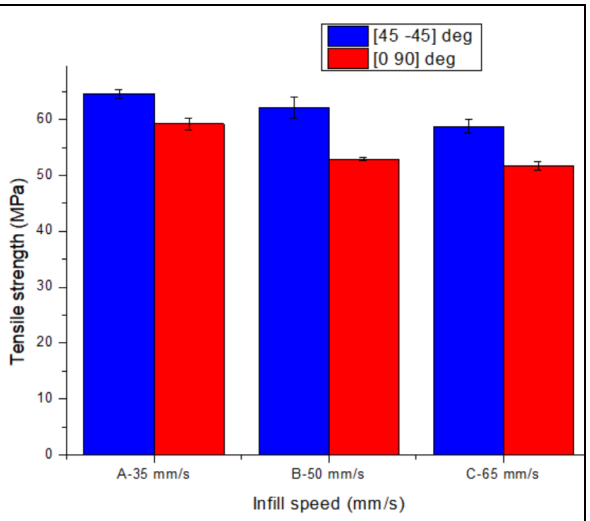

Figure 5: Tensile strength

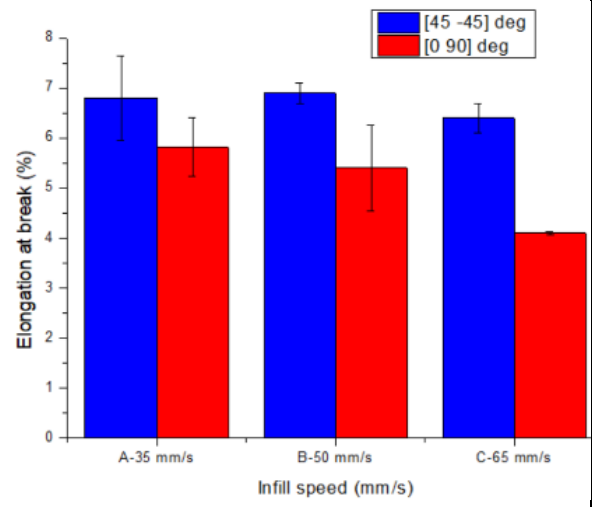

Figure 6: Value of Elongation at break.

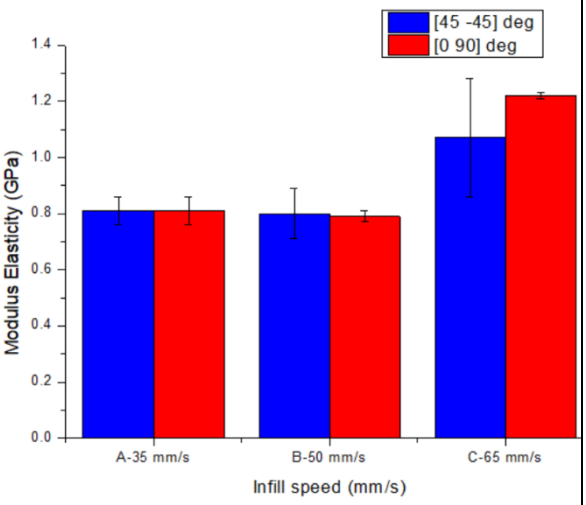

Figure 7: Modulus of elasticity

a

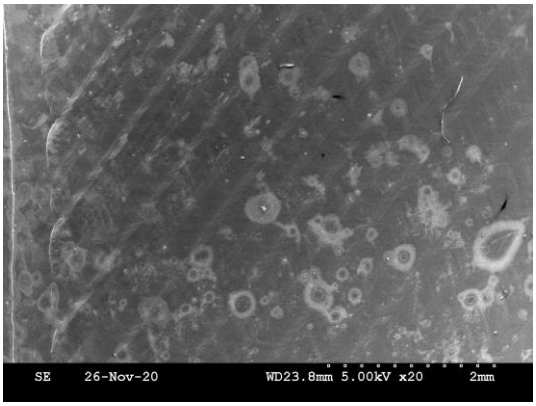

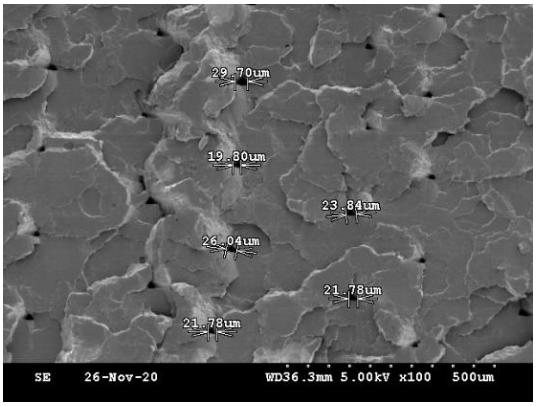

Raster angle 45°/- 45°, In-fill speed 35 mm/s

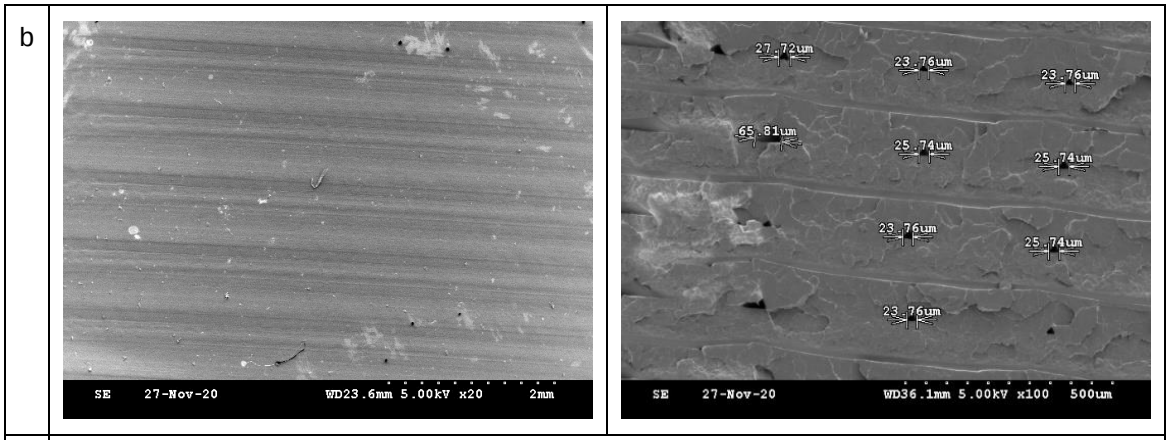

Figure 8: SEM images shows the defects in 3D printing parts.

Moreover, the average value of each parameter across its different levels were utilised to create the main effect graphs. The most effective combination for optimal results was identified through the highest average values for these parameters. The analysis of variance (ANOVA) was used to observe the influence of each parameter on mechanical properties. This analysis reveals both the primary and the combined influences of the process parameters on tensile strength. The primary effect refers to the direct influence of individual parameters, whereas the interaction effect represents the combined influence of two independent parameters on tensile strength. Figure 9 displays the primary effect of 3D printing process parameters on the mechanical properties of the samples. It is evident from the plot that the peak tensile strength corresponds to the raster angles of 45°/-45°. The analysis of the mean further indicates that as infill speed increases, tensile strength tends to decrease. Figure 10 illustrates the interaction effects of the parameters, averaging out the means across all dual-factor combinations. If two lines intersect on the plot, this suggests potential interplay between the two associated factors *[39]*. However, as indicated in Figure 10, no interaction seems to exist between the infill speed and the raster angles. With a raster angle set at 45°/-45°, a superior tensile strength is consistently observed across all infill speed levels. This indicates that raster angle plays a more significant role in influencing tensile strength than does infill speed. These observations align with the experimental findings discussed earlier.

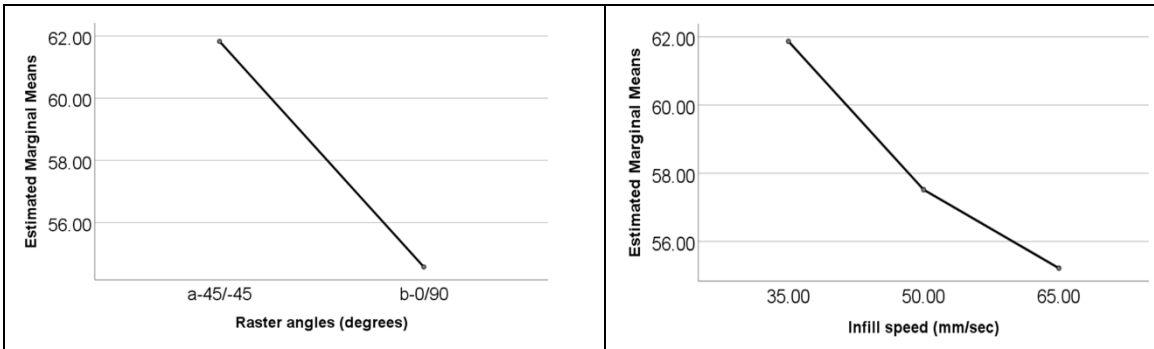

(a) (b)

Figure 9: Main effect of 3D printing process parameters on tensile strength (a) Raster orientation (b) Infill speed.

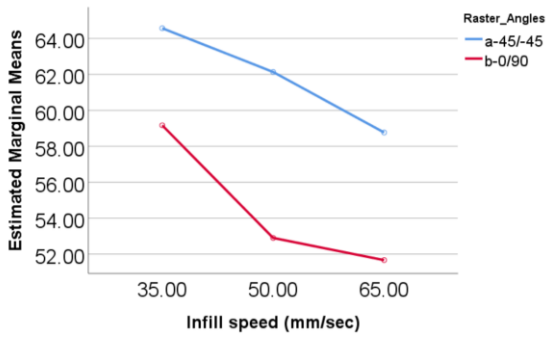

(a) Infill speed*Raster angle

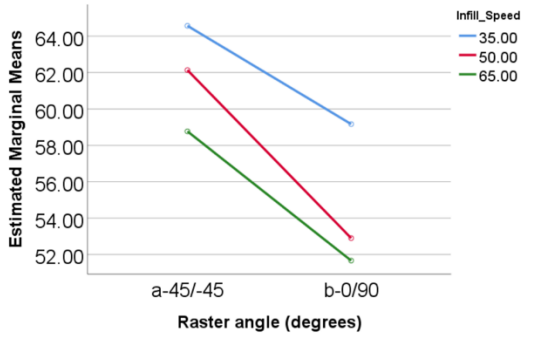

(b) Raster angle*Infill speed

Figure 10: Interaction effort of process parameters on tensile strength.

Moreover, it is imperative to determine which parameter notably affects the material strength of the samples. ANOVA (analysis of variance) was used to identify the most significant parameters in terms of in percentage affecting the response parameter. The p-value indicates the statistical significance of individual parameters. Taguchi et al. [40] have noted that, for a confidence level of 95%, the p-value should be below 0.05. The ANOVA results for the average tensile strength data are provided in Table 3. For raster angle, P-value is 0.001 which is considerably less than the typical p value of 0.05. This suggests that the effect of raster angles on the tensile strength is statistically significant. In addition to the partial Eta Squared for raster angle is 0.600, This indicates that raster angles account for approximately 60% of the variance in the tensile strength, after accounting for other factors. Such a high value means that raster angles have a strong and practically significant influence on the material strength. For infill Speed, P-value is 0.023 which is less than 0.05, suggesting that the effect of infill speed on the tensile strength is statistically significant. Moreover, Partial Eta Squared for infill speed is 0.465 reveals that infill speed accounts for about 46.5% of the variance in the tensile strength when other factors are controlled for. This suggests that infill speed also has a considerable and practically relevant impact on the strength. For the interaction of Raster Angles and Infill Speed, P-value is 0.665. This relatively high p-value suggests that the interaction between raster angles and infill speed does not significantly influence the strength, at least at the typical 0.05 alpha level. The Partial Eta Squared for this interaction is 0.066 that indicates a small effect size for the interaction. This suggests that, while there might be some interaction effect, its magnitude is minimal, accounting for only about 6.6% of the variance in the strength. Hence, both raster angles and infill speed independently have significant effects on the strength, with raster angles having a slightly stronger effect than infill speed. However, the interaction between raster angles and infill speed does not significantly influence the material strength.

Table 3: Analysis of Variance for Material strength.

Source	*Type III Sum of Squares*	*df*	*Mean Square*	*F*	*p value*	*Partial Eta Squared*
Corrected Model	384.107[a]	5	76.821	5.852	0.006	0.709
Intercept	60970.320	1	60970.320	4644.375	0.000	0.997
Raster angles	236.169	1	236.169	17.990	0.001	0.600
Infill speed	136.870	2	68.435	5.213	0.023	0.465
Raster angles x Infill speed	11.068	2	5.534	0.422	0.665	0.066
Error	157.533	12	13.128			
Total	61511.960	18				
Corrected Total	541.640	17				

a. R Squared = 0.709 (Adjusted R Squared = 0.588)

Third experiment

The two aforementioned studies demonstrated that a raster angle of 45°/- 45° and an infill speed of 30 mm / sec are the optimal 3D printing parameters for PLA. In this experiment, it is reasonable to assume that the chosen printing parameters, specifically a raster angle of 45°/-45° and an infill speed of 30 mm/sec, are applicable across various materials to assess their impact and determine if they are also suitable for other 3D printing materials. To validate their universality, these parameters were applied to five different 3D printed materials, maintaining a consistent experimental setup with 100% infill density, 0.1 mm infill layer thickness, and recommended bed and extrusion temperatures specified by manufacturers. Additionally, this study was undertaken to establish a standardised benchmark for 3D printing settings across various materials.

The 3D printing materials PETG, PLA tough, Recycle PLA, Plain PLA, and ABS are used for this study, as illustrated in Figure 11. The mechanical attributes of these materials were assessed and compared with the manufacturer's recommended properties [41]. For each material type, three identical tensile samples were printed, resulting in a total of 15 samples. All these 3D printed samples were tested based on the standard testing method ASTM D638, utilising the Universal testing machine, consistent with the procedures used in previous experiments.

Figure 12 and Figure 13 present a comparison of the observed tensile strength and modulus of elasticity values against the manufacturer-recommended values for these materials. ABS, PETG, and tough PLA exhibit higher tensile strength values, showcasing improvements of 5%, 16%, and 44%, respectively, while these are marginally lower for PLA and recycled PLA. Notably, the three aforementioned materials align well with the printed parameters, exceeding the manufacturer's recommended values. However, the situation is different when considering tensile modulus. In this aspect, all tested materials record values below the manufacturer's recommendations, indicating a less rigid behaviour than what was anticipated that could be due to several factors such as the testing conditions, the quality of the raw materials used, and the manufacturing process. It is important to note that the manufacturer’s values are based on ideal conditions and may not always reflect the real-world performance of the material. The tensile modulus reflects the material's resistance to deformation under tensile stress, and lower values suggest a more flexible material. Despite falling short of the manufacturer's suggestions, this reduced stiffness can be advantageous in certain engineering applications where flexibility and resilience are desired characteristics. Therefore, the experimental outcomes reveal both strengths and potential benefits in specific applications due to the observed deviations in tensile properties.

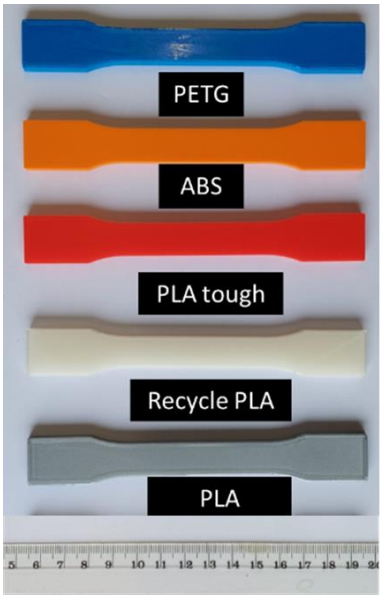

Figure 11: Tensile test samples for five different materials

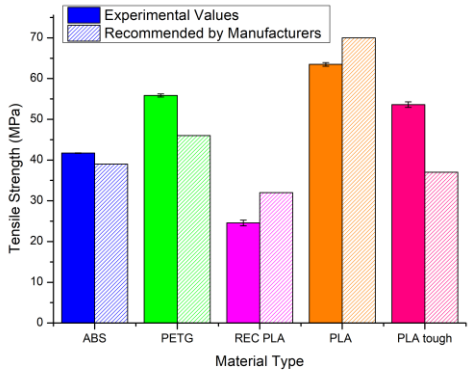

Figure 12: A comparison of tested tensile strength values against manufacturer-recommended values for the various materials.

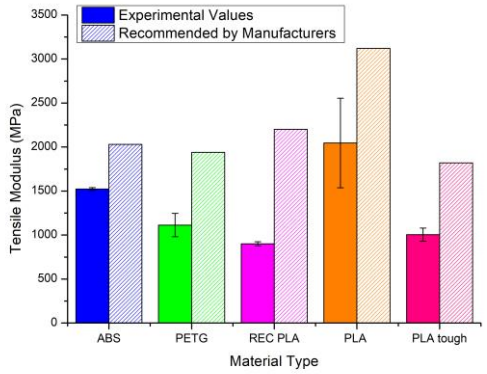

Figure 13: A comparison of tested Modulus of elasticity values against manufacturer-recommended values for the various materials.

Conclusion

In this study, three experimental studies were performed. The initial two sets of experiments aided in refining the values of two crucial parameters in the 3D printing process: raster orientation and infill speed for PLA material. Following the results of these experiments, the optimised values of these parameters were used for other five materials in order to establish a standardised benchmark for 3D printing settings across various materials for these parameters. The printed parts were assessed using a tensile test. Furthermore, a Scanning Electron Microscopy (SEM) analysis was conducted on both the fracture interface after tensile testing and the outer surfaces of these samples to elucidate material failure modes and reasons. The study yields the following conclusions.

Both experimental and analysis of variance (ANOVA) results proposed that both raster angles and infill speed independently have significant effects on the strength, with raster angles having a slightly stronger effect than infill speed. However, the interaction between raster angles and infill speed does not significantly influence the material strength. Moreover, the exploration of optimal 3D printing parameters for PLA, namely a raster angle of 45°/- 45° and an infill speed of 30 mm/sec, provided significant insights into their applicability across various other 3D printing materials. This study utilised five specific materials: PETG, PLA tough, Recycle PLA, Plain PLA, and ABS. Through systematic testing, it was determined that ABS, PETG, and tough PLA displayed better tensile strength, even surpassing the benchmarks set by their respective manufacturers using the optimal 3D printing parameters. Interestingly, Plain PLA and Recycled PLA showed slightly lower tensile strengths, yet still held value in certain applications. When examining the tensile modulus, a consistent trend was observed across all materials: they exhibited less rigidity than what the manufacturers recommended. This extra flexibility can be useful for many engineering applications where a balance between strength and flexibility is advantageous. while the research provides valuable insights into the effects of raster angles and infill speed on material strength for a specific set of materials, caution should be exercised when extending these findings to other materials or when applying different printing parameters. Further research encompassing a wider array of materials and mechanical properties is essential to enhance the robustness and generalisability of the conclusions drawn in this study.

Acknowledgements

The experiments were conducted at the University of Sunderland, and the author expresses gratitude to the university for providing funding to support this research. Special thanks are extended to Mr. Alistair MacDonald and David Winter for their contribution to fabricating the 3D printed samples for the experiments. Additionally, appreciation is extended to Ms. Kayleigh Ironside for her support and assistance in conducting the SEM work.

References

1. Utela B, Storti D, Anderson R, Ganter M (2008) A review of process development steps for new material systems in three dimensional printing (3DP). Journal of Manufacturing Processes 10:96–104

2. Gupta N, Weber C, Newsome S (2012) Additive manufacturing: status and opportunities. Science and Technology Policy Institute, Washington

3. Gebhardt A (2011) Understanding additive manufacturing

4. Altaf K, Rani AMA, Raghavan VR (2013) Prototype production and experimental analysis for circular and profiled conformal cooling channels in aluminium filled epoxy injection mould tools. Rapid Prototyping Journal

5. Vaezi M, Chianrabutra S, Mellor B, Yang S (2013) Multiple material additive manufacturing – Part 1: a review. Virtual and Physical Prototyping 8:19–50. https://doi.org/10.1080/17452759.2013.778175

6. Bachmann J, Schmölzer S, Ruderer MA, et al (2022) Photo-differential scanning calorimetry parameter study of photopolymers used in digital light synthesis. SPE Polymers 3:41–53. https://doi.org/10.1002/pls2.10063

7. Shi Q, Yu K, Kuang X, et al (2017) Recyclable 3D printing of vitrimer epoxy. Materials Horizons 4:598–607

8. Tian X, Liu T, Wang Q, et al (2017) Recycling and remanufacturing of 3D printed continuous carbon fiber reinforced PLA composites. Journal of cleaner production 142:1609–1618

9. Sanchez FAC, Lanza S, Boudaoud H, et al Polymer Recycling and Additive Manufacturing in an Open Source context: Optimization of processes and methods. 11

10. Ivanova O, Williams C, Campbell T (2013) Additive manufacturing (AM) and nanotechnology: promises and challenges. Rapid Prototyping Journal

11. Durakovic B (2018) Design for additive manufacturing: Benefits, trends and challenges. Periodicals of Engineering and Natural Sciences 6:179–191

12. Novakova-Marcincinova L, Novak-Marcincin J, Barna J, Torok J (2012) Special materials used in FDM rapid prototyping technology application. In: 2012 IEEE 16th International Conference on Intelligent Engineering Systems (INES). IEEE, Lisbon, Portugal, pp 73–76

13. Dudek P (2013) FDM 3D printing technology in manufacturing composite elements. Archives of Metallurgy and Materials 58:1415–1418

14. Muthe LP, Pickering K, Gauss C (2022) A Review of 3D/4D Printing of Poly-Lactic Acid Composites with Bio-Derived Reinforcements. Composites Part C: Open Access 8:100271. https://doi.org/10.1016/j.jcomc.2022.100271

15. Dizon JRC, Gache CCL, Cascolan HMS, et al (2021) Post-Processing of 3D-Printed Polymers. Technologies 9:61. https://doi.org/10.3390/technologies9030061

16. Wu N, Zhang H (2017) Mechanical properties and phase morphology of super-tough PLA/PBAT/EMA-GMA multicomponent blends. Materials Letters 192:17–20. https://doi.org/10.1016/j.matlet.2017.01.063

17. Hashima K, Nishitsuji S, Inoue T (2010) Structure-properties of super-tough PLA alloy with excellent heat resistance. Polymer 51:3934–3939. https://doi.org/10.1016/j.polymer.2010.06.045

18. Kai CC, Fai LK, Chu-Sing L (2003) Rapid prototyping: principles and applications in manufacturing. World Scientific Publishing Co., Inc., Singapore

19. Cui X, Jar P-YB (2023) Prediction of quasi-static elastic modulus for polyethylene-terephthalate-glycol prepared from fused deposition modeling. SPE Polymers 4:49–62. https://doi.org/10.1002/pls2.10085

20. Kechagias J, Zaoutsos S (2024) Effects of 3D-printing processing parameters on FFF parts' porosity: outlook and trends. Materials and Manufacturing Processes 0:1–11. https://doi.org/10.1080/10426914.2024.2304843

21. Kechagias J, Chaidas D (2023) Fused filament fabrication parameter adjustments for sustainable 3D printing. Materials and Manufacturing Processes 38:933–940. https://doi.org/10.1080/10426914.2023.2176872

22. Moser N, Strasser C, Tanda A, et al (2024) Influence of printing direction and filler orientation on the thermal conductivity of 3D printed heat sinks. SPE Polymers 5:83–94. https://doi.org/10.1002/pls2.10112

23. Naveed N (2021) Investigating the Material Properties and Microstructural Changes of Fused Filament Fabricated PLA and Tough-PLA Parts. Polymers 13:1487

24. Comb J, Priedeman W, Turley PW (1994) FDM® Technology process improvements. In: 1994 International Solid Freeform Fabrication Symposium. Austin, United States

25. Sanatgar RH, Campagne C, Nierstrasz V (2017) Investigation of the adhesion properties of direct 3D printing of polymers and nanocomposites on textiles: Effect of FDM printing process parameters. Applied Surface Science 403:551–563

26. Mohamed OA, Masood SH, Bhowmik JL (2015) Optimization of fused deposition modeling process parameters: a review of current research and future prospects. Advances in Manufacturing 3:42–53

27. Chadha A, Ul Haq MI, Raina A, et al (2019) Effect of fused deposition modelling process parameters on mechanical properties of 3D printed parts. World Journal of Engineering 16:550–559. https://doi.org/10.1108/WJE-09-2018-0329

28. Chin Ang K, Fai Leong K, Kai Chua C, Chandrasekaran M (2006) Investigation of the mechanical properties and porosity relationships in fused deposition modelling-fabricated porous structures. Rapid Prototyping Journal 12:100–105

29. Dudescu C, Racz L (2017) Effects of raster orientation, infill rate and infill pattern on the mechanical properties of 3D printed materials. ACTA Univ Cibiniensis 69:23–30

30. Wu W, Geng P, Li G, et al (2015) of layer thickness and raster angle on the mechanical properties of 3D-printed PEEK and a comparative mechanical study between PEEK and ABSInfluence. Materials 8:5834–5846

31. Fatimatuzahraa AW, Farahaina B, Yusoff WAY (2011) The effect of employing different raster orientations on the mechanical properties and microstructure of Fused Deposition Modeling parts. In: 2011 IEEE Symposium on Business, Engineering and Industrial Applications (ISBEIA). IEEE, Langkawi, Malaysia, pp 22–27

32. Letcher T, Waytashek M (2014) Material property testing of 3D-printed specimen in PLA on an entry-level 3D printer. In: ASME 2014 international mechanical engineering congress and exposition. American Society of Mechanical Engineers, Montreal, Canada, p V02AT02A014-V02AT02A014

33. Naveed N (2020) Investigate the effects of process parameters on material properties and microstructural changes of 3D-printed specimens using fused deposition modelling (FDM). Materials Technology 0:1–14. https://doi.org/10.1080/10667857.2020.1758475

34. Pulipaka A, Gide KM, Beheshti A, Bagheri ZS (2023) Effect of 3D printing process parameters on surface and mechanical properties of FFF-printed PEEK. Journal of Manufacturing Processes 85:368–386. https://doi.org/10.1016/j.jmapro.2022.11.057

35. D20 Committee Test Method for Tensile Properties of Plastics. ASTM International

36. Sood AK, Ohdar RK, Mahapatra SS (2010) Parametric appraisal of mechanical property of fused deposition modelling processed parts. Materials & Design 31:287–295

37. Alhazmi MW, Backar AH (2020) Influence of Infill density and Orientation on the Mechanical Response of PLA+ Specimens Produced using FDM 3D Printing. International Journal of Advanced Science and Technology 29:3362–3371

38. Mazumder M, Ahmed R, Ali AW, Lee S-J (2018) SEM and ESEM techniques used for analysis of asphalt binder and mixture: A state of the art review. Construction and Building Materials 186:313–329

39. Rajpurohit SR, Dave HK (2019) Analysis of tensile strength of a fused filament fabricated PLA part using an open-source 3D printer. Int J Adv Manuf Technol 101:1525–1536. https://doi.org/10.1007/s00170-018-3047-x

40. Taguchi G, Chowdhury S, Wu Y (2004) Taguchi's Quality Engineering Handbook. (No Title). https://doi.org/10.1002/9780470258354

41. Material Archive. In: UltiMaker. https://ultimaker.com/materials/. Accessed 8 Oct 2023